SMAR 2017 – Fourth Conference on Smart Monitoring,
Assessment and Rehabilitation of Civil Structures

SMAR 2017

Active shear strengthening of RC beams using shape memory alloys

Joan Rius[1], Antoni Cladera[1], Carlos Ribas[1] and Benito Mas[1]

[1] University of Balearic Islands, Palma (Mallorca), Spain

ABSTRACT: Shear failure of reinforced concrete (RC) members is brittle, with little or no warning. For this reason, it is always necessary to avoid this type of failure, and shear strengthening of existing structures is sometimes required due to previous design mistakes, to adapt them to a change in the use of the structure or to fulfil new code requirements. In this paper, the results of an experimental campaign designed to proof the possibility of using the shape memory effect of shape memory alloys (SMA) to externally strengthen shear critical beams will be presented. Two different configurations will be discussed: a pseudo-rectangular spiral and U shape with steel plates. The SMA used in this experimental work was Ni-Ti-Nb, although similar configurations could be designed with other SMAs. The experimental results show a promising performance of the proposed technology, increasing the shear strength and the deflection at failure of the retrofitted beams.

1 INTRODUCTION

Shear failures in RC members are associated with brittle collapses, which may cause material and human losses. Therefore, it is necessary to avoid this type of failure, and shear strengthening of existing structures is often needed due to different causes. The strengthening technologies for critical shear beams may be classified in two categories: passive strengthening and active strengthening methods. In the first ones (e.g. using FRP), the strengthening increases the safety of the structure and its strength in front of future actions but it is necessary that the strengthened structure increases its deformation and its level of damage to allow the strengthening material to work. However, in active strengthening methods, the structures are directly prestressed or actively confined when the strengthening material is placed.

In this paper, a new active strengthening technology for shear critical beams will be presented using the shape memory effect of Shape Memory Alloys (SMA). In terms of structural engineering, SMAs have three key properties (Otsuka and Wayman 1998): shape memory effect, pseudoelasticity and damping capacity. The shape memory effect is the key property for the featured strengthening technology, and it refers to the phenomenon whereby SMAs are capable of returning to a predefined shape upon heating. If this recovery strain is constrained, because the SMA is used, for example, to wrap a beam, the SMA will generate recovery stresses when heated and cooled afterwards, prestressing and/or confining the concrete member.

Binary Ni-Ti alloys are the market dominant alloy, with many applications in different engineering fields. However, as will be seen later on this paper, its narrow thermal hysteresis

make this alloy not appropriate for its use in prestressing applications using the shape memory effect in civil engineering structures. Ni-Ti-Nb alloys are easier to handle and store due to its larger temperature hysteresis (Melton, Proft, and Duerig 1989; Melton, Simpson, and Duerig 1986). This allows the material to be prestrained at low temperature and be safely transported at ambient temperatures, activated, and keeping high values of recovery stresses for ambient temperatures. The cost of Ni-Ti-Nb is very high, but recent research on iron-based shape memory alloys (Cladera et al. 2014) envisages the application of cheaper shape memory alloys with very similar behavior. These iron based shape memory alloys have already satisfactorily been used for the flexural strengthening of RC beams embedding them in a shotcrete layer (Shahverdi, Czaderski, Annen, et al. 2016) or as near-surface mounted reinforcement (Shahverdi, Czaderski, and Motavalli 2016). In any case, despite the high cost of Ni-Ti-Nb, the amount of material needed is small and should be placed only in critical regions of the beams, so this application promises a very interesting technology for the strengthening of key civil infrastructures.

In real engineering practice, the objective of strengthening a RC beam in shear would be to avoid the shear failure, forcing the shear strength to be higher than the flexural strength and, consequently, inducing a more ductile flexural failure. However, to be able to quantify the shear strengthening with the proposed technology, the objective in the experimental campaign presented in this paper will be to raise the shear strength but without reaching the flexural strength.

2 EXPERIMENTAL PROGRAM

2.1 Tested beams and properties of steel and concrete

Twenty reinforced concrete (RC) small scale beam specimens were produced, all with the same geometry and longitudinal reinforcement, although in this paper 8 beams will be presented. The beam specimens has been selected to summarize the observed behavior.

The RC beam specimens were 80 mm wide, b, and 150 mm deep, h (Figure 1). The total length of the beam specimens was 900 mm, and the tests were carried out with a central point load. The shear span, a, was equal to 340 mm, with a/d approximately equal to 2.68, where d is the effective depth (d= 127 mm). The characteristics of the beams are summarized in Table 1. Two identical specimens were tested each time to ensure the repeatability of the test results.

Standard 150 mm cubes and 150 mm × 300 mm cylinders were cast with the specimens to obtain the compressive strength, f_{cm}, and the splitting strength, f_{sp}, respectively. Maximum aggregate size of 14 mm was used. The cubes and cylinders were kept under the same environmental conditions as the beam specimens until the time of testing the beams. Longitudinal reinforcement was composed of ϕ16 mm standard B500SD rebars (A_s = 201 mm^2). Both ends of the bars were welded to a plate to guarantee sufficient anchorage in such small beam specimens. The mechanical properties of the longitudinal bars are: f_y = 513 MPa, f_u = 642 MPa, ε_u = 20.5%.

Beams 1.1. and 1.2 are reference beams, only with longitudinal reinforcement and they were not externally strengthened. Beams 2.1 and 2.2 (Figure 2) were externally strengthened using an external pseudo-spiral with pitch equal to 100 mm (except the last segment, with a pitch equal to 75 mm). Beams 3.1a and 3.2a were identical to beams 2.1 and 2.2 but the externally placed pseudo-spirals were not activated. These beams (3.1a and 3.2a) were tested only for academic reasons, to really proof the benefit of using the shape memory effect of the Ni-Ti-Nb. Finally, beams 8.1 and 8.2 were externally strengthened using the Ni-Ti-Nb wire in a U-configuration (Figure 2), mechanically fixed with steel plates. The spacing of the wires was 100 mm, except for the last one (75 mm).

Table 1. Details of the beam specimens.

Beam no.	f_{cm} (MPa)	f_{sp} (MPa)	Shear strengthening			
			ϕ/spacing (mm)	*Ni-Ti-Nb state*	φ_{front} (°)	φ_{back} (°)
1.1 – Reference	41.4	3.2	-	-	-	-
1.2 – Reference	41.7	3.2	-	-	-	-
2.1 - Sϕ3/100/UCR/A	41.9	3.2	ϕ3/100	Activated	90	56
2.2 - Sϕ3/100/UCR/A	42.1	3.2	ϕ3/100	Activated	90	56
3.1a - Sϕ3/100/UCR/NA	42.6	3.3	ϕ3/100	Non-Activated	90	56
3.2a - Sϕ3/100/UCR/NA	42.6	3.3	ϕ3/100	Non-Activated	90	56
8.1 - Uϕ3/100/UCR/A	39.7	3.4	ϕ3/100	Activated	90	90
8.2 - Uϕ3/100/UCR/A	39.7	3.4	ϕ3/100	Activated	90	90

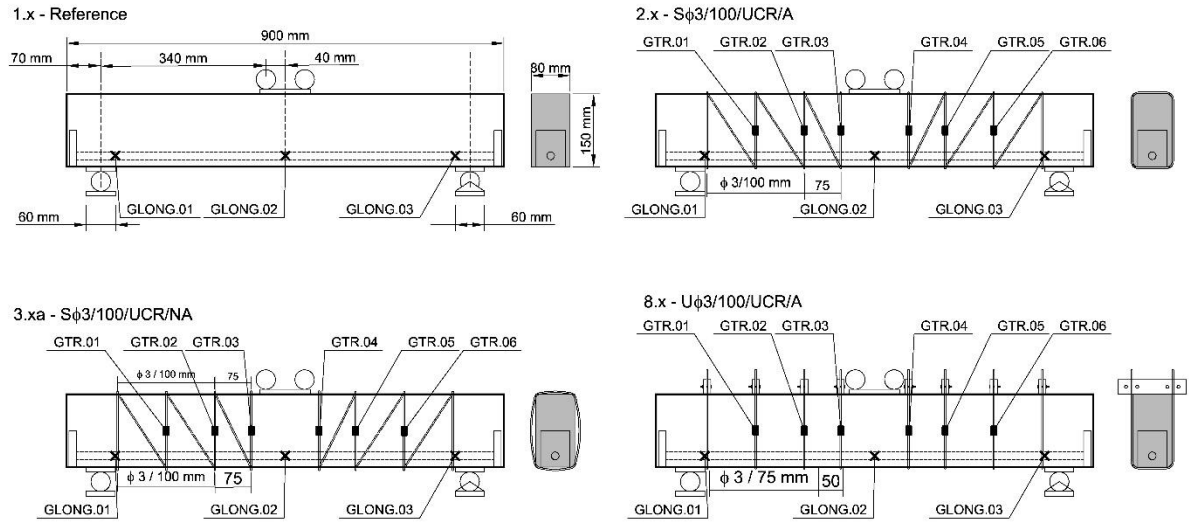

Figure 1. Beam geometry.

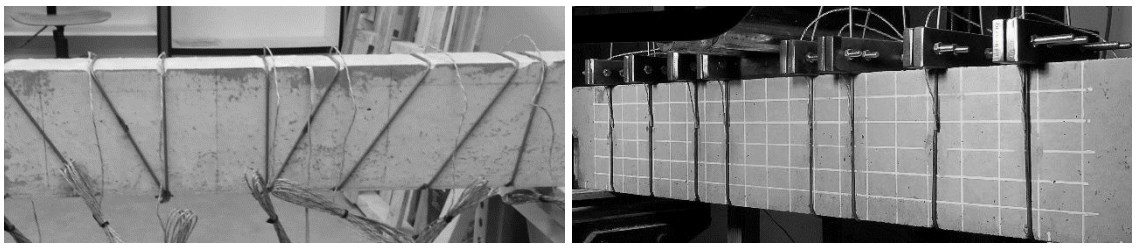

Figure 2. View of two beam specimens: pseudo-spiral strengthening and U-shape strengthening.

2.2 Ni-Ti-Nb wire key properties

3 mm-diameter Ni-Ti-Nb wires were used without indentations of any type. A Ni-Ti-Nb sample was analyzed through energy dispersive X-ray spectroscopy (EDX) to determine its composition, resulting in Ti at.45.81%, Ni at.45.76% and Nb at.8.43%.

The transformation temperatures were determined using two experimental techniques: Differential Scanning Calorimetry (DSC) and electrical resistance tests. The transformation

temperatures measured with the last technique were equal to: M_f = - 135 ºC, M_s = -105 ºC, A_s = 69 ºC and A_f = 74 ºC, for the first thermal cycle. A second thermal cycle was carried out obtaining the same M_f and M_s temperatures, but in the second cycle, A_s = -45 ºC and A_f = -21 ºC. This reduction of the thermal cycle is beneficial for this application: once the SMA has been transported to the working place, installed and activated, the alloy will remain in austenite phase.

Figure 3 presents a stress recovery tests. The Ni-Ti-Nb sample is heated in the thermal chamber up to 200 ºC, the temperature is kept constant and then is cooled. The position control test is performed with an initial pre-load of around 8 MPa, and the load cell measured the stresses generated to keep constant the position of the crossbar. The recovery stresses obtained after heating to 200 ºC the sample, and cooling it afterward, was approximately 560 MPa. The temperature of the wire was monitored using 5 thermocouples. Note that during the cooling process the stress increased until reaching a plateau just at the end. This increase is due to the couple effect of the thermal contraction of the clamps.

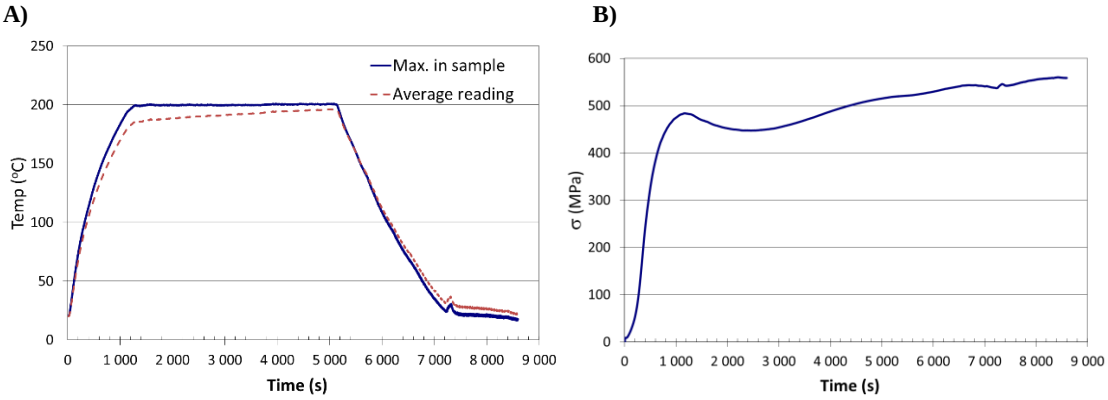

Figure 3. Stress recovery test. A) Temperature vs. time. B) Stress vs time.

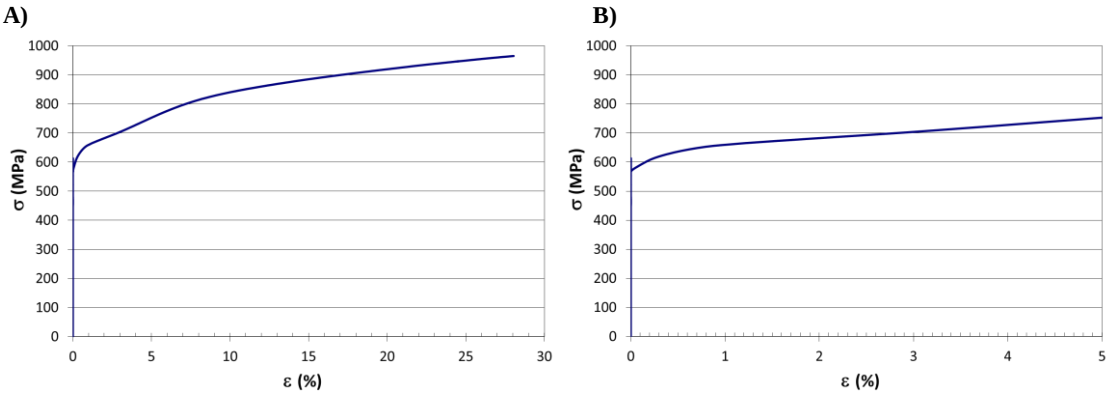

Figure 4. Stress–strain behavior at ambient temperature of the Ni-Ti-Nb wire after stress-recovery test. A) Full test. B) Zoom of the first part of the diagram. The vertical line for ε = 0 % correspond to the stress-recovery test (strain constrained).

After performing the recovery stress tests, and without unloading the sample, a conventional stress-strain test was performed, with the results shown in Figure 4. The ultimate stress was approximately 965 MPa for a strain of around 28%. The tangent modulus of elasticity at the beginning of the tensile test after activating the SMA with constrained strain (with the initial stress of the tensile test was 25 GPa, although the modulus decreased above a stress of 650 MPa.

3 TEST RESULTS

All the reported beams failed in shear. Figure 5 and Table 2 summarize the most important results. It may be clearly seen that the effectivity of placing the pseudo-spiral around the beam but without activating it (beams 3.1a and 3.2a) is negligibly and the response of these beams is very similar to the response of the reference beams (beams 1.1 and 1.2). The shear strength and the deflection at failure is very similar for beams 1.1, 1.2, 3.1a and 3.2a.

However, when the strengthening material is activated (2.1, 2.2, 8.1 and 8.2), the strengthening method is clearly effective, almost doubling the shear strength respect to the shear strength of the reference beams. The behavior for the beams with the pseudo-spiral (2.1 and 2.2) and with the U-shape strengthening (8.1 and 8.2) is quite similar, with larger deflections at failure but not a clear increase on ductility. This is a remarkable difference respect to the use of Ni-Ti pseudo-spirals as internal reinforcement, which was found to provide ductile shear failures (Mas, Cladera, and Ribas 2016).

It can be observed in Figure 5 that the differences in the geometry of the strengthening do not change the final strength of the beams. It should be noted that the pseudo-rectangular spiral reinforcement confines horizontally the reinforced member (2.1 and 2.2) the U shape reinforcement with the steel plate does not (8.1 and 8.2). Note also that pseudo-rectangular spiral reinforcement need more SMA reinforced material that U shape reinforcement.

The crack patterns after the peak load in the tested beams are shown in Figure 6, confirming that all beams failed in shear. The strains measured in the longitudinal reinforcement in beams 1.2, 2.2, 3.2a and 8.2 are shown in Figure 7. The plots for the corresponding beams x.1 are very similar and they are not shown for brevity. For the beams without external strengthening or the spiral not activated (beams 1.2 and 3.2a) in Figure 7, the longitudinal reinforcement did not yield. For the strengthened beams, only the strain gauged located near the support in the span where the failure took place yielded, confirming the shear failure without steel yielding at midspan.

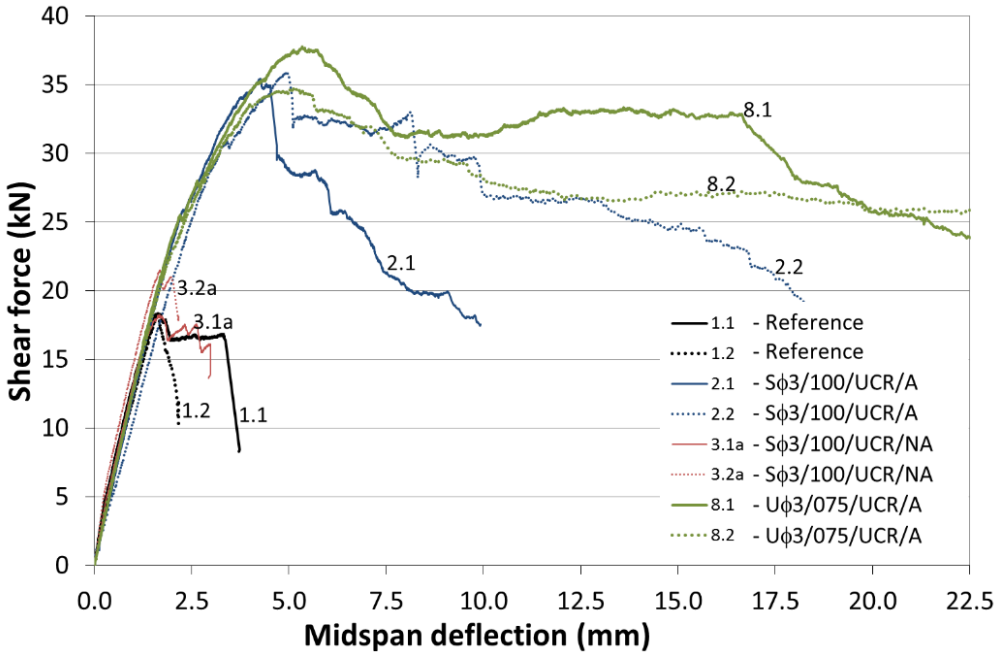

Figure 5. Load vs. deflection for tested beam specimens.

Table 2. Summary of test results.

Beam no.	V_{test} *(kN)*	δ at V_{test} *(mm)*	l/δ *(-)*
1.1 - Reference	18.30	1.59	479
1.2 - Reference	18.41	1.64	462
2.1 - Sϕ3/100/UCR/A	35.41	4.26	178
2.2 - Sϕ3/100/UCR/A	35.95	4.94	154
3.1a - Sϕ3/100/UCR/NA	18.23	1.67	456
3.2a - Sϕ3/100/UCR/NA	21.47	1.69	450
8.1 - Uϕ3/100/UCR/A	37.74	5.35	142
8.2 - Uϕ3/100/UCR/A	34.75	5.15	148

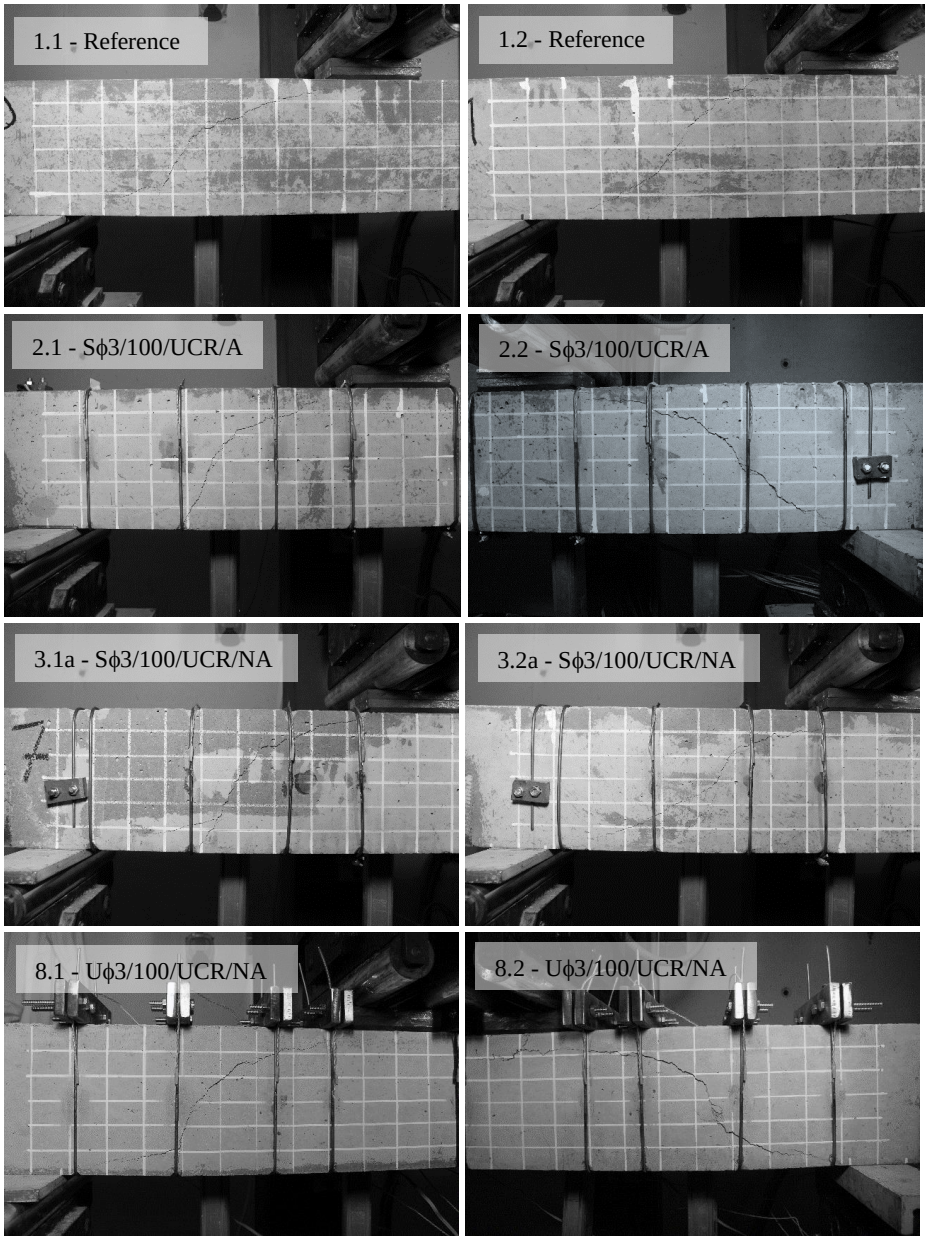

Figure 6. Crack patterns after peak load.

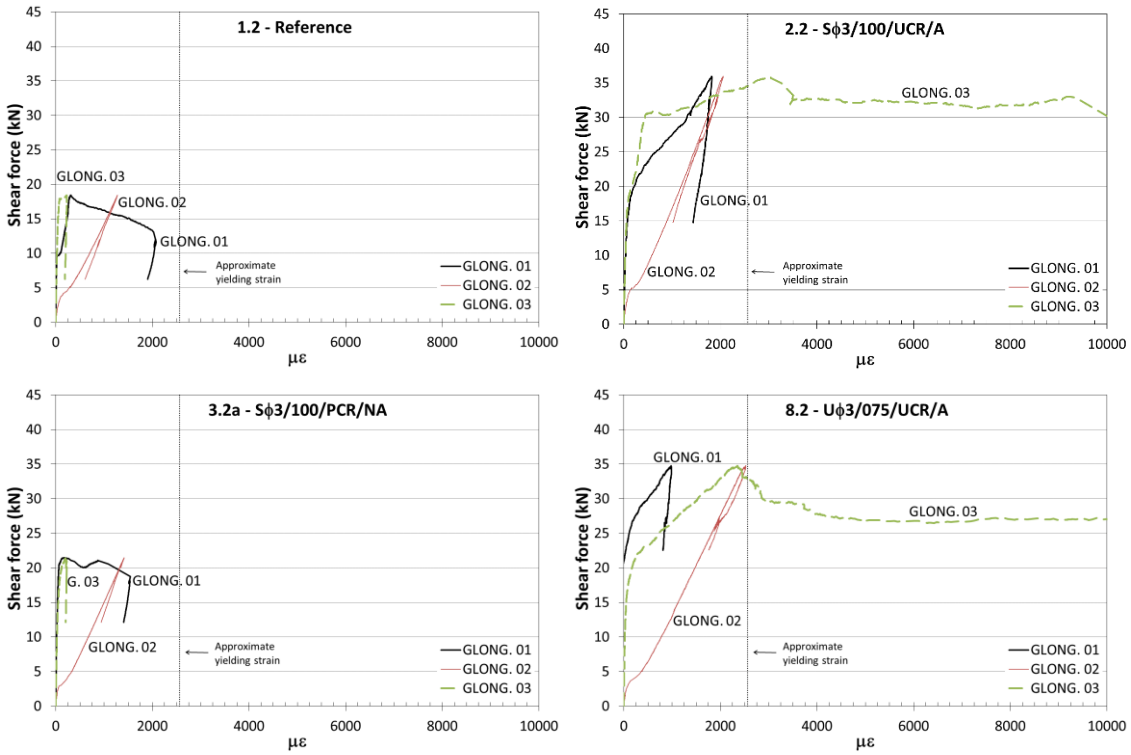

Figure 7. Strains measured in the longitudinal reinforcement in beams 1.2, 2.2, 3.2a and 8.2.

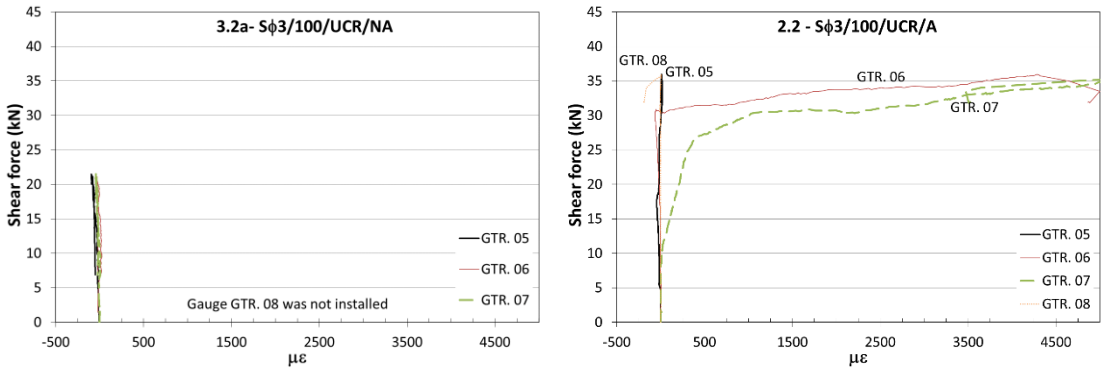

Figure 8. Strains measured in the external reinforcement in beams 3.2a and 2.2.

Finally, Figure 8 presents the strains at the external shear reinforcement for the beam 3.2a (non-activated) and for beam 2.2. The geometry of the external spiral was the same, but in case of placing it without generating recovery stresses (beam 3.2a) the spiral did not correctly confine the beam and the wire did not increase its deformation when the shear damage increased.

4 CONCLUSIONS AND FUTURE WORK

An experimental campaign focused on assessing the possibility of strengthening critical shear beams by means of a shape memory alloy with shape memory effect has been performed. The experimental results show a promising performance of the proposed technology, increasing the shear strength of the retrofitted beams and the deflection at failure when the strengthening

material is correctly placed and activated to generate recovery stresses by means of the shape memory effect. It has been observed that strengthening with pseudo-rectangular spiral reinforcement and U shape reinforcement with the steel plate has similar results, although the last one needs less SMA material. This research was planned as a proof-of-concept experimental campaign and more research is needed. The cost of Ni-Ti-Nb is very high, but the recent production of Fe-based SMA materials specifically oriented to structural concrete industry will boost the research and the real applications due to their reasonable cost and excellent properties.

5 ACKNOWLEGMENTS

This research was developed in the framework of projects BIA2015-64672-C4-3-R (AEI / FEDER, UE) and BIA2012-31432 (MINECO / FEDER, UE).

6 REFERENCES

Cladera, A., Weber, B., Leinenbach, C., Czaderski, C., Shahverdi, M., and Motavalli, M., 2014, Iron-based shape memory alloys for civil engineering structures: an overview. *Construction and building materials*, 63, 281-293.

Mas, B., Cladera, A., and Ribas, C., 2016, Experimental Study on Concrete Beams Reinforced with Pseudoelastic Ni-Ti Continuous Rectangular Spiral Reinforcement Failing in Shear. *Engineering Structures* 127:759–68.

Melton, K. N., Proft, J. L., and Duerig, W., 1989, Wide Hysteresis Shape Memory Alloys Based on the Ni-Ti-Nb System. *MRS Int'l. Mtg. on Adv. Mats. Vol 9.* Pp. 165–70.

Melton, K. N., Simpson, J., and Duerig. W., 1986, A New Wide Hysteresis NiTi Based Shape Memory Alloy and Its Applications. P*roceedings of the International Conference on Martensitic Transformations. ICOMAT-86*, Pp. 1053–58.

Otsuka, K. and Wayman C. M., 199, *Shape Memory Materials*. United Kingdom: Cambridge University Press.

Shahverdi, M., Czaderski, C., Annen, P., and Motavalli, M., 2016, Strengthening of RC Beams by Iron-Based Shape Memory Alloy Bars Embedded in a Shotcrete Layer. *Engineering Structures* 117:263–73.

Shahverdi, M., Czaderski, C., and Motavalli, M., 2016, Iron-Based Shape Memory Alloys for Prestressed near-Surface Mounted Strengthening of Reinforced Concrete Beams. *Construction and Building Materials* 112:28–38.